New constraints on the thermal and volatile evolution of Mars

Alice Guest, Suzanne E. Smrekar

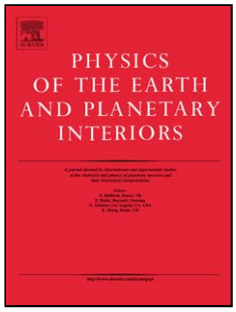

Title: New constraints on the thermal and volatile evolution of Mars

Authors: Alice Guest, Suzanne E. Smrekar

PII: S0031-9201(07)00141-0
DOI: doi:10.1016/j.pepi.2007.06.010
Reference: PEPI 4848

To appear in: *Physics of the Earth and Planetary Interiors*

Received date: 14-5-2006
Revised date: 4-6-2007
Accepted date: 19-6-2007

Please cite this article as: Guest, A., Smrekar, S.E., New constraints on the thermal and volatile evolution of Mars, *Physics of the Earth and Planetary Interiors* (2007), doi:10.1016/j.pepi.2007.06.010

NEW CONSTRAINTS ON THE THERMAL AND VOLATILE EVOLUTION OF MARS

Alice Guest* and Suzanne E. Smrekar,

Jet Propulsion Laboratory, California Institute of Technology
4800 Oak Grove Dr., MS 183-501, Pasadena, CA 91106, USA
fax: (818) 393-5059
e-mail: alice.guest@seznam.cz, (corresponding author)
e-mail: ssmrekar@jpl.nasa.gov, ph. (818) 354-4192

*now at: Dept. for Geo- and Environmental Sciences, LMU München, Luisenstr. 37, 80333 München, Germany

Abstract

The thermal and volatile evolution of Mars has not been studied from the perspective of consistency with the preservation of the Martian global dichotomy and estimates of the elastic thickness over time. We use three thermal evolution models for Mars: 1) stagnant lid, 2) early plate tectonics followed by stagnant lid, and 3) mantle overturn, to calculate the amount of relaxation of the dichotomy boundary and elastic thickness values for Noachian- and Hesperian-aged terrains. To explore a wide range of parameters, we evaluate two different initial mantle temperatures, and wet and dry rheologies. Our model results show that the relative water content of the crust has an effect roughly equal to 500 K variations of initial mantle temperature. For all

three thermal models, a lower crust viscosity of 10^{20}-10^{21} Pas during the first 0.1 Ga after formation of dichotomy would allow for the preservation of the long-wavelength topography of Mars and fitting of the elastic thickness. This viscosity range implies either wet, cold (~1500 K) lower crust, or dry, hot (~2000 K) lower crust in Noachian. Additional constraints are necessary to distinguish between the individual thermal models. For the stagnant lid model, neither the cold, wet crust nor the hot, dry crust agree with timing and amount of the crustal production (Hauck and Phillips, 2002). Moreover, drying of the crust is required for this model in order to match the admittance elastic thickness at the Hesperian/Amazonian boundary implying remelting of the crust. The hot, dry crust in the early plate tectonics model limits a plate tectonic epoch to only 100-200 Myr and implies dry mantle, which is in disagreement with water found in meteorites. The cold, wet crustal rheology implies the formation of crust during the plate tectonics regime because of the low crustal production during the stagnant lid regime. For mantle overturn, the temperature required for wet crust does not fit the original mantle profile while the dry crust does; however in order to explain the initially hot thermal profile the crust must have been emplaced very fast. Generally, dry crustal rheology does not fit low elastic values in the Hesperian and implies either that rheology may differ between the southern and northern hemispheres: wet in northern hemisphere and dry in southern hemisphere, or that local weakening occurred. Wet crustal rheology fits well all elastic data except S. Hellas rim, which may be anomalous. Mantle rheology is unconstrained by our modeling and can be either dry or wet.

Key words: Mars, elastic thickness, thermal evolution, water, relaxation modeling

47

48 **Introduction**

49

50 The thermal and volatile evolution of Mars has important implications for the production
51 of the Martian crust, relaxation of Martian topographic features, evolution of elastic thickness,
52 and generation of the magnetic field. Several models for the thermal evolution of Mars have
53 been proposed. The simplest model for cooling of Mars, the stagnant lid convection model (e.g.,
54 Hauck and Phillips, 2002), predicts the crustal production and preservation of the topographic
55 features on Mars (Guest and Smrekar, 2004, 2005), but does not predict magnetic field
56 generation without superheating of the core. A model that includes an early epoch of plate
57 tectonics followed by stagnant lid convection (Nimmo and Stevenson, 2000; Breuer and Spohn,
58 2003) can explain the generation of the magnetic field without superheating (Nimmo and
59 Stevenson, 2000), but cannot predict the crustal production within the lifetime of a dynamo.
60 Another type of cooling model for Mars is based on a thermodynamical model of initial magma
61 ocean crystallization (Elkins-Tanton et al., 2003). This model predicts two melt reservoirs, in
62 agreement with the estimated volume and early formation of the Martian crust (e.g., Solomon et
63 al., 2005).

64 There is evidence that the Martian volatile content has changed over the history of Mars
65 (Jakosky and Phillips, 2001). The water content in the mantle and crust can change due to
66 volcanism, as was suggested for the Tharsis region during the Noachian to Hesperian, where the
67 formation of valley networks and large outflow channels were formed by an extensive amount of
68 water on the surface, probably released during volcanic activity (e.g., Greeley, 1987, Jakosky
69 and Phillips, 2001, McSween et al., 2001, Phillips et al., 2001, Solomon et al., 2005). However,

the presence of water in the crust or mantle at 175 Ma (McSween et al., 2001) suggests that the loss of the water was either partial or local.

The thermal and volatile evolution of Mars has not been examined using constraints from the preservation of the Martian dichotomy and estimates of the elastic thickness over time. Each of the thermal evolution models has a different initial thermal state and rate of cooling of the lithosphere and thus has a different effect on the preservation of the topography and elastic thickness evolution. The general cooling history of the lithosphere is preserved in the elastic thickness estimates from the gravity/topography admittance. The loss of water from the interior would influence the strength of the crust and/or mantle and thus influence the relaxation of the topography and evolution of the elastic thickness.

The major topographic feature on Mars, the Martian dichotomy, has been preserved since its formation at 4.13 Ga or earlier (Solomon et al., 2005; Frey, 2006) . The Martian dichotomy is characterized by differences in elevation of ~ 5 km (Frey et al., 1998) and in crustal thickness of ~30 km (Zuber et al., 2000; Neumann et al., 2004) between the northern and southern hemispheres. The Martian dichotomy was emplaced, when the planet was still relatively hot. It is thus surprising that the dichotomy elevation and crustal thickness difference did not completely relax early in Martian history. Partial modification of the Martian dichotomy, which was suggested for the Ismenius area (Guest and Smrekar, 2005) and other regions (Nimmo, 2005) occurred prior to ~ 3.9-3.1 Ga based on geological studies (McGill and Dimitriou, 1990; Tanaka et al., 1992). In any case, insignificant or partial modification of the boundary suggests a relatively rapid cooling of the planet. The evolution of the elastic lithosphere based on the gravity/topography admittance (McGovern et al., 2002, 2004) shows an increase of elastic thickness from < 15 km in the Noachian (~ 4 Ga) to at least 110 km at the Hesperian/Amazonian

93 boundary (~ 3 Ga) also suggesting relatively fast cooling. In this paper we examine whether
94 preservation of the dichotomy boundary and an increase of the elastic thickness are in accord
95 with any of the three thermal evolution models and whether the volatile evolution played a role.
96 Here we use three models of lithospheric cooling based on three different thermal
97 evolution models of Mars to model changes in elastic thickness and the long-term preservation of
98 the Martian dichotomy. We test both wet and dry rheologies in the crust and mantle in order to
99 provide constraints on both the thermal and interior volatile evolution of Mars. We model
100 relaxation across the dichotomy boundary from the Noachian to the Hesperian/Amazonian using
101 semi-analytical viscoelastic numerical modeling with two density and three viscosity layers
102 (Guest and Smrekar, 2005). Our results are compared to the topography across the dichotomy
103 boundary and to elastic thickness estimates derived from gravity and topography data
104 (McGovern et al., 2002, 2004; Belleguic et al., 2005; Hoogenboom and Smrekar, 2006).
105
106
107 **Thermal Models**
108
109 We use three models of the cooling of the lithosphere: stagnant lid, early plate tectonics
110 and mantle overturn (Figure 1). The three thermal models represent distinct lithospheric cooling
111 histories. The stagnant lid model starts with the coolest lithosphere, but does not cool as
112 efficiently as the other two models. The early plate tectonics and mantle overturn models cool
113 with similar efficiency, even though the mantle temperature evolutions differ significantly.
114 The stagnant lid model assumes cooling of the interior through an immobile lid on top of
115 a convecting mantle. It is based on a stagnant-lid coupled thermal-magmatic convection model

for Martian mantle and crust (nominal model of Hauck and Phillips, 2002). Key elements of the Hauck and Phillips (2002) model are the inclusion of the energetics of melting, a wet (weak) mantle rheology, self-consistent fractionation of heat-producing elements to the crust, and a near-chondritic abundance of those elements.

In the early plate tectonics model, the planet's interior cools efficiently during the active plate tectonic regime and warms up after the transition to the stagnant lid regime. The early plate tectonics model is based on convection models of Breuer and Spohn (2003) and Spohn et al. (2001) that study the temperature evolution in the Martian interior assuming an early epoch of plate tectonics followed by single-plate tectonics with stagnant lid mantle convection. When plate tectonics stops at 4 Ga, the initially thin lithosphere significantly thickens during the first 1 Gyr causing cooling of the lithosphere and warming of the mantle. The transition from plate tectonics to a stagnant lid regime is assumed to occur at 4 Ga when the magnetic field is estimated to have shut down (Connerney et al., 1999; Breuer and Spohn, 2003).

Temperature for the mantle overturn model is based solely on the thermodynamic data that predict an inverse thermal gradient (hot on top, cold at the bottom) following mantle overturn in the Martian interior. The model is based on the thermodynamic calculations of Elkins-Tanton et al. (2003) corrected for the heat of fusion during melting (Elkins-Tanton et al., 2005). This model predicts a temperature distribution in the Martian interior after mantle overturn that is caused by unstable cumulate density stratification related to the crystallization of a magma ocean that forms due to the energy of accretion. Mantle overturn brings the hot temperature close to the surface and cold temperature to the bottom of the mantle almost instantaneously. Precise timing of this model is unclear. However, the latest work by Elkins-Tanton et al. (2005) indicates that the crust created by the overturn is emplaced within 50 Myr

after accretion of the planet. Based on the convection model of Zaranek and Parmentier (2004), the mantle will cool conductively for 100-300 Myr after the overturn; mantle convection may or may not initiate subsequently depending on the initial viscosity. The limiting viscosity may be on the order 10^{18} Pa s or less. If mantle convection does occur, our results are valid only up to 100-300 Myr.

We determine cooling of the lithosphere by solving the heat conduction equation in the lithosphere using the initial and boundary conditions based on constraints from the original thermal evolution models (see also Guest and Smrekar (2005) for details of the thermal modeling). These constraints are the evolution of the thickness of the thermal lithosphere, defined as a conductive lid, and the evolution of the temperature at the base of the lithosphere. We model cooling of the lithosphere for 1 Ga, based on an estimate of the maximum time needed for relaxation and on the estimated age of the southern highlands for which elastic thickness estimates exist (McGovern et al., 2002, 2004). Unless otherwise noted, the average global crustal thickness in each model is 62 km.

For the stagnant lid model, we use the nominal model of Haucks and Phillips (2002) that best fits the observations for Mars. In this model, 75 % of the 62 km thick crust forms by ~ 4 Ga which is used as a starting point in our model. This model includes radiogenic heating. The initial thermal gradient in the crust of ~18 K/km at 4 Ga (Figure 1a) is determined by solving the heat conduction from 4.5 to 4 Ga. From 4 to 3 Ga, the thermal gradient decreases from 18 to 13 K/km. The mantle cools only about 60 K, but because of the conductive lid thickening, the temperature at 100 km cools by 300 K. The cooling rate is constant in time.

For the early plate tectonics model, our starting point is 4 Ga when plate tectonics has stopped. The early plate tectonics model fails to generate the observed crustal thickness of at

least 50 km during the stagnant lid regime and therefore requires that the entire crust was emplaced during the plate tectonics epoch. We adopt the model from Spohn et al., 2001, which is similar to the model EPT21 from Breuer and Spohn (2003), with an initial mantle viscosity of ~ 10^{21} Pa s. As an initial condition, we assume a linear increase of temperature with depth in the 62-km-thick crust from 220 K to 1728 K (a thermal gradient of 24.3 K/km). The mantle warms up by 230 K after the start up of the stagnant lid regime (see also Lenardic et al., 2004) in the convection model, but because of the stagnant lid thickening, the temperature at a depth of 100 km cools by 800 K (Figure 1b), faster than in the stagnant lid model without plate tectonics (Hauck and Phillips, 2002). Therefore, the end of plate tectonics is reflected in the shallow lithosphere (~50 km) by an increased cooling rate. Cooling is fastest during the first 250 Myr.

For the mantle overturn model, we assume a conductive cooling of the reversed temperature profile after mantle overturn which may have occurred as early as 50 My after accretion (Elkins-Tanton et al., 2005). As an initial condition in the crust, we assume a linear temperature increase with depth from 220 K to 1790 K (thermal gradient of 25.3 K/km). Temperature cools by about 200 K in the mantle and by 750 K at 100 km during 1 Gyr (Figure 1c). Cooling is very fast during the first 250 Myr. The cooling of the lithosphere in this model is similar to the cooling in the early plate tectonics model.

Our models of lithosphere cooling are simplified versions of the thermal models, especially the plate tectonics and mantle overturn models, for which we make assumptions about crustal thickness, radiogenic heating, and initial thermal gradient. We use a crustal thickness of 62 km. This value is predicted by the stagnant lid model and is within the model uncertainties of the other two thermal models and thus allows for a comparison of the models results. The distribution of the radiogenic heating is not specified for the plate tectonics and mantle overturn

185 models and so we neglect it in our modeling. Therefore, the initial thermal gradient in the crust is
186 not specified for these models and we assume the simplest option, the linear thermal gradient. As
187 a consequence, our crust is cooler than it would be with the radiogenic heating included. The
188 initial thermal gradient is high because of the initially thin lithosphere. In order to test for
189 uncertainties in the model parameters, for each of the three thermal models (in the following text
190 termed "warm mantle" variant) we construct a temperature profile with a 200 K cooler mantle
191 temperature (termed "cold mantle" variant). This variation in mantle temperature results in a
192 100-200 K difference in the temperature at the base of the crust, and simulates possible
193 variations in thermal gradient and radiogenic heating.
194
195
196 **Relaxation and elastic-thickness modeling**
197
198 We model the topographic and crustal relaxation of the dichotomy boundary in the 4500
199 km long cross-section through the boundary (Figure 2). The vertical dimension of the model is
200 3000 km. Our model consists of two layers of different density materials, crust and mantle, and
201 three viscosity layers. The initial topography and crust-mantle boundary relief, in the Cartesian
202 coordinate system, are described using geometric functions of sin and cos and are thus dependent
203 only on the horizontal distance and time.
204 We simulate topographic relaxation using a semi-analytical model (Guest and Smrekar,
205 2005) in which we solve the same equations as in the model of gravity-driven relaxation of a
206 topographic load at the surface of a density-stratified incompressible fluid (Grimm and Solomon,
207 1988, Appendix A), except for the coordinate system (Cathles, 1975). In this method, the

208 horizontal variations of stress and displacement are transformed to the frequency domain with a
209 Fourier transform (Cathles, 1975) while the vertical variations are integrated numerically using a
210 fourth-order Runge-Kutta method thus allowing for vertical variations of viscosity. We solve the
211 time-dependence of the coupled topographic decay on the surface and the crust-mantle boundary
212 by integrating velocity at the boundaries over the time step. We solve for two characteristic
213 deformation modes associated with two density interfaces. We update the boundary topographies
214 after each time step and solve the equilibrium and constitutive equations again. Such a time
215 stepping allows for accommodation of viscosity changes with time. The viscosity variations with
216 depth and time must be input in the semi-analytical model a priori at each time step.

217 In order to incorporate time changes in viscoelasticity, a Laplace transform is applied on
218 the constitutive equation of the incompressible viscous fluid (Zhong, 1997, Equation A1). The
219 transformed equation has the same mathematical form as the constitutive equation for the
220 incompressible viscous fluid if the viscosity that is input in the solution is expressed as:

221

222 $$\eta_s = \eta/(1+s\tau), \qquad (1)$$

223

224 where η_s is viscosity dependent on the Laplace transform variable, η is viscosity calculated
225 using only creep strain rate (representing a viscous fluid), s is the Laplace transform variable,
226 and τ is the relaxation time defined in our calculations as $\tau = \eta/3G$, where G is rigidity. The
227 Laplace transform variable s is equivalent to the reciprocal value of time t, which is numerically
228 integrated over the time of calculations (0-1 Gyr) in seconds. If t is significantly smaller than τ,
229 then the value of η_s is decreased in comparison to the value η (see Equation 1). This decrease in
230 viscosity can be understood as being caused by the increased importance of the elastic strain rate,

and thus for small times we obtain a viscoelastic solution. If t is near or higher than τ, then value of η_s is near the value η, and viscous solution is obtained. In this way, our numerical solution for viscous fluid becomes a solution for the viscoelastic fluid. This method was tested against benchmarks of Zhong (1997) (see Guest and Smrekar, 2005).

Viscosity is updated in the model before each time step ($\eta = \sigma/2\dot{\varepsilon}$, where $\dot{\varepsilon}$ is strain rate based on the creep laws shown in Table 1, and σ is stress). Because strain rate is dependent on temperature and stress, viscosity varies continuously with depth and time. While temperature is based on the three thermal models, it is impossible to predict the stress variations for all depths over 1 Gyr because stress evolves during the relaxation depending on the rheology used. Based on comparison of the semi-analytical modeling with the finite-element modeling (details in Guest and Smrekar, 2005), we simplify the depth dependence of viscosity into three layers, initially consisting of the viscosity of the upper crust, lower crust and mantle. The depth of the boundary between the crust and mantle is fixed, whereas the boundary between upper and lower crust evolves with time depending on the depth location of viscosity of 10^{29} Pa s. The later boundary divides the elastic and viscoelastic part of the lithosphere, initially located in the crust. When this boundary reaches the mantle due to lithospheric cooling, the three layers become elastic crust, elastic mantle (both with the same viscosity) and viscoelastic mantle. Therefore, the time evolution of only four parameters is needed for our calculations: viscosity of the elastic layer, viscosity of the lower crust, viscosity of the mantle and depth of the elastic layer. The viscosity of the elastic layer, represented by a value of 10^{29} Pa s, is constant with time. The time evolution of the viscosity for lower crust and mantle is based on the stress estimates that are described in brief below. The description of the location of the depth of the elastic thickness is given later in the chapter.

The relaxation of stress in the lower crust is difficult to predict. For strong rheologies (dry, cold and warm temperature), we assume zero strain rate changes in the layer. The stress evolution is then solved in small time steps from time 0 till calculation time t assuming an exponential decay of stress in time (Turcotte and Schubert, 2001) and temperature change with time. For weak rheologies (wet, cold and warm temperature), we assume a strong lower crustal flow, similar to the flow in the mantle. The viscosity in the lower crust is then the same as viscosity in the mantle. Only the stress at the bottom of the layer is necessary to predict for our calculations, because the viscosity at the bottom of the lower crust successfully represents the viscosity of the whole lower crust (shown in Guest and Smrekar, 2005). Stress in the mantle is essentially constant (0.12 MPa) and mantle viscosity changes mainly due to temperature changes. The viscosity in the mantle is represented by the viscosity value just below the base of the thermal lithosphere for the stagnant lid and plate tectonics models. For the mantle overturn model, we use the depth of 150 km because the base of the thermal lithosphere, defined as a conductive lid, would be thicker than 250 km which is too deep to influence the relaxation of the dichotomy boundary. The depth of 150 km is close to the depth of the thermal lithosphere in the other two models during first 300 Myr when most of the relaxation happens. Therefore, the mantle viscosity is higher and relaxation is smaller than if we used a 250 km thick thermal lithosphere. This choice of depth does not influence the elastic thickness modeling.

The values of mantle and lower-crustal viscosities input in the relaxation models are shown in Figure 3. These values are taken at the bottom of the conductive layer (as shown on Figure 1) for first two models and at depth of 150 km for the mantle overturn model. The viscosity of the upper elastic layer is always 10^{29} Pa s. The mantle viscosity at the beginning of calculations is the same for the stagnant lid and early plate tectonics models and is one order of

277 magnitude higher for the mantle overturn model. Mantle viscosity increases by a factor of five
278 during 1 Gyr for the stagnant lid model. For the early plate tectonics model, mantle viscosity
279 decreases by two orders of magnitude during 1 Gyr due to heating of the planet's interior. For
280 the mantle overturn model, mantle viscosity increases by one order in 100 Myr and at least by
281 ten orders in 1 Gyr. The viscosity in the lower crust for dry rheology increases by four to seven
282 orders during first 100 Myr in all three models. This is caused by fast relaxation of stress in the
283 layer. We use the same viscosity in the lower crust and in the mantle if wet rheology is used.

284 The location of the elastic boundary in the crust, defined by viscosity of 10^{29} Pa s, is
285 based on the thermal evolution as shown on Figure 1 and the stress distribution in the southern
286 hemisphere of the model. The initial deviatoric stress distribution in the crust is caused by the
287 elevation and crustal-thickness differences between the northern lowlands and southern
288 highlands (calculation time 0). The initial values of 2 MPa at the surface to 20 MPa at the base of
289 crust are based on finite element modeling. Early in time, the stress in the lower crust (defined
290 as having a viscosity $<10^{29}$ Pa s) relaxes and redistributes to the elastic part of the crust. The
291 viscosity difference due to the stress increase in the elastic crust is, however, insignificant in
292 comparison to changes resulting from the temperature gradient and therefore the elastic thickness
293 does not change. When cooling becomes significant (around 10-100 Myr), the base of the elastic
294 crust migrates downward. The stress distribution stays locked within the elastic upper crust and
295 does not change, but in the meantime, stress decreased via viscous relaxation in the lower crust.
296 The stress drop in the lower crust results in a more rapid increase of viscosity causing a more
297 rapid increase in the thickness in the elastic layer than would result from the decrease in
298 temperature alone. When the bottom of the elastic layer reaches the mantle, the thickness of the

299 layer increases due to a change of the rheological law and a stress drop with temperature being a
300 minor effect.

301 When wet crustal rheology is used, two separate elastic layers, consisting of a layer in the
302 crust and a layer in the mantle, will develop. In such a case the effective elastic thickness is
303 determined using (Burov and Diament, 1995):

304 $$Te = \sqrt[3]{h_1^{\,3} + (h_2 - h_c)^3}\,, \qquad (2)$$

305 where Te is the effective elastic thickness, h_1 is the depth of the elastic thickness in the crust, h_c
306 is the crustal thickness and h_2 is the depth of the elastic thickness in the mantle. If the elastic
307 thickness in the crust (h_1) is the same as the elastic thickness in the mantle ($h_2 - h_c$) then
308 $Te = 1.26h_1$. The thickening of the elastic layer is shown on Figure 4 and discussed in more
309 detail under Results.

310 The uncertainties in stress evolution introduce uncertainties into the viscosity predictions.
311 Using a simple viscosity profile also results in small errors in prediction of topographic
312 relaxation (Guest and Smrekar, 2005). For this reason, we will distinguish only three stages of
313 relaxation in our results: no relaxation, partial relaxation and complete relaxation, even though
314 our technique provides more precise results. Despite the challenges inherent in analytic models
315 of viscosity evolution, our approach newly includes the time evolution of viscosity and elastic
316 thickness, and is therefore better suited for modeling of the effects of cooling of the lithosphere
317 than the other studies (Zhong, 1997; Nimmo and Stevenson, 2001; Nimmo, 2005).

318

319 **Input Parameters**

320

Input parameters that influence the relaxation of the dichotomy boundary are the highland elevation, dichotomy boundary slope, crustal thickness, and creep laws. We assume an initial highlands elevation of 5 km that is isostatically compensated by a crustal root of 24 km (Figure 2). The initial slope of the dichotomy boundary is two degrees, slightly higher than present-day observations (Frey et al., 1998). The average crustal thickness for Mars is estimated to be greater than 45 km (Neumann et al., 2004) and lower than 80 km (Nimmo and Stevenson, 2001). In our models, we use an average crustal thickness of 62 km, yielding values of 47 km and 77 km in northern plains and southern highlands, respectively. We use this value because it is predicted by the stagnant lid thermal model and is also consistent with the other two thermal models. Our rheology is based on creeps laws determined during laboratory experiments (Table 1). For a wet crust, we use the creep law determined with undried specimens of diabase (Caristan, 1982), while for dry crust samples are dried prior to deformation (Mackwell et al., 1998). Similarly for mantle flow laws, water-free and water-saturated conditions were used on olivine, the most abundant and probably the weakest mineral of peridotites. (Karato and Wu, 1993). The density of crust is 2900 kgm^{-3}, and the density of mantle is 3500 kgm^{-3} (Zuber et al., 2000). The Young's modulus and Poisson's ratio are 1.e11 Pa and 0.5, respectively, for both crust and mantle.

Elastic Thickness Data

We use estimates of elastic thickness for local areas of different ages (McGovern et al., 2002, 2004; Hoogenboom and Smrekar, 2006, Belleguic et al., 2005) as a general constraint on

elastic thickness with time. McGovern et al. (2002, 2004) use admittance to calculate elastic thickness for 15 regions located mostly on southern hemisphere of Mars. These regions have surface ages ranging from the Noachian to Amazonian (Figure 4), and are either located in the old cratered terrain of the southern highlands or consist of large volcanic provinces. Although these regions have had distinct geologic histories, they show a trend of increasing elastic thickness with time that very likely reflects the overall cooling of the planet (e.g., Solomon and Head, 1990; McGovern et al., 2002). Elastic thickness estimates in the northern lowlands, except Elysium Rise and Alba Patera, are problematic and were not included in the analysis of McGovern et al. (2002, 2004). The elastic thickness for four regions in the northern plains in the Noachian was estimated by Hoogenboom and Smrekar (2006). Their values range from 0-45 km with an overlap in 10-25 km. The values for Alba Patera and Elysium Rise in the Hesperian-Amazonian were recalculated by Belleguic et al. (2005) with an improved method that gives slightly higher values that those given by (McGovern et al., 2004). The age of the regions is constrained only roughly.

In a later section we compare our estimates of elastic thickness from thermal models to those derived from admittance. To avoid confusion we refer to values derived from gravity and topography data as 'admittance estimates' to distinguish them from the estimates predicted by our thermal models. The areas which represent each epoch and that we try to fit with our modeling are: the Noachian terrains with an elastic thickness up to 25 km, Solis Planum of Hesperian age and elastic thickness of ~ 30 km, and Hesperian-Amazonian chasmata with elastic thicknesses higher than ~ 60-100 km. All these regions are located in the vicinity of Tharsis in the southern hemisphere and should therefore experience similar thermal evolution. The fit to Alba Patera and Elysium Rise, located in the northern hemisphere, will be discussed separately

as well as the fit to the South Hellas Rim. It should be noted that most of the observations were made on the southern hemisphere, where the crustal thickness is higher than our average thickness (but this is appropriate for our models).

A few caveats are worth considering when attempting to fit 'admittance elastic thickness'. One possible uncertainty is that the surface age might not reflect the time of loading. For example, one hypothesis is that a broad scale plume caused removal of the lower crust under the northern plains (Zhong and Zuber, 2000). In such a case the elastic thickness may have been reset without altering the surface age. Or, the time of loading could be older than surface age. Areas of very significant volcanic activity, such as Elysium and Tharsis, might have reset the elastic thickness due to the sustained volcanic activity, however modeling of such a problem confirms that the elastic thickness reflects the general decrease of heat flux predicted for Mars by thermal models (Dombard and Phillips, 2005).We concur with McGovern et al.'s (2002) assessment that the increase in elastic thickness with time reflects global cooling. However we do not try to match their values of elastic thickness precisely due to the caveats above. The features with the largest admittance elastic thickness estimates are the Valles Marineris Chasmata and the South Hellas Rim with intrusion that are all modeled with bottom loading. The bottom loading tends to give larger values that top loading models (e.g., Petit and Ebinger, 2000) but certainly can't be responsible for the very large differences in the values.

Results

Elastic thickness

For each thermal model, we predict the thickening of the elastic lithosphere using combinations of wet or dry mantle and crustal rheologies, and warm or cold mantle temperature variations. We do not consider the combination wet crust/dry mantle because we are uncertain about the prediction of stresses in the relaxation modeling due to the lack of the experience with finite-element modeling for this case. However, we treat this possibility in the Discussion section.

The predicted elastic thickness for the stagnant lid model between 4 and 3 Ga is shown in Figure 4a. When wet rheology is used in both the crust and mantle, the stagnant lid model predicts an elastic thickness of 20 km in the Noachian for both the warm and cold mantle temperatures. In the Hesperian and at the Hesperian/Amazonian (H/A) boundary, the mantle elastic layer develops, but is only a few km thick and thus does not significantly influence the effective elastic thickness. The effective elastic thickness is 30 km in the Hesperian and less then 40 km at H/A boundary (using Equation 2, h1=30 km, h2=80 km, hc=62 km). When dry rheology is used in the crust and mantle, the elastic thickness is 40 km (both warm and cold variants) in the Noachian, 60 km (warm variant) and 90 km (cold variant) in the Hesperian and 85 km (warm variant) and 110 km (cold variant) and at H/A boundary. When dry crust and wet mantle rheologies are used, the elastic thickness is 40 km (warm and cold variants) in the Noachian, 60-70 km (warm and cold variants) in the Hesperian and 60 km (warm variant) and 80 km (cold variant) and at H/A boundary. We do not show the elastic thickness for wet crust and dry mantle, but they can be estimated from Figure 4a using the curves for wet rheology and for dry mantle: the double elastic layer develops with the effective elastic thickness in the Hesperian

40 km, and 55 km at the H/A boundary for both cold and warm variants. Generally, the increase of the elastic thickness at 3.8 Ga is caused by the stress drop between the upper and lower crust and the increase of the elastic thickness above 62 km related to the change of rheology.

Both early plate tectonics and mantle overturn models have similar evolution of elastic thickness (Figure 4 b,c) to each other, only shifted in time. For wet crustal and mantle rheology, the elastic thickness is 15-20 km (for both warm and cold variant) in the Noachian that reaches 30-40 km after 0.2 Gyr. A double elastic layer develops in 0.5 Gyr (3.5 Ga for early plate tectonics, 3.9 Ga for mantle overturn) with an effective elastic thickness of 50 km (warm variant) and 65 km (cold variant). The elastic thickness is 120 km (warm variant) and 160 km (cold variant) during the Hesperian-Amazonian for both models. When dry crustal rheology, and dry or wet mantle rheologies are used, elastic thickness quickly increases from 30 km (both warm and cold variants) in the Noachian, to 80-120 km (warm variant) or 100-170 km (cold variant) in 0.5 Ga (Hesperian for early plate tectonics, Late Noachian for mantle overturn, to 120-180 km (warm variant) or 110-220 km (cold variant) in the Hesperian-Amazonian. For the mantle overturn model, when wet crustal and mantle rheologies and cold temperature are used, the elastic thickness increases from 60 km to 160 km at 3.7 Ga (cold mantle variant) because of the change of rheology and a stress drop between the lower crust and mantle (Figure 4c). Specifically, to a depth of 62 km, the crustal rheology determines the elastic thickness, below which the mantle rheology determines the elastic thickness. If we consider a higher crustal thickness of 77 km in the southern hemisphere, then the sharp increase in elastic thickness would occur when the elastic thickness reaches 77 km. When the elastic thickness exceeds the crustal thickness, then it follows the mantle curve for the appropriate rheology. By combining the

435 appropriate curves with desired crustal thickness, various elastic thickness evolutions can be
436 made.

437 For all three thermal models in Noachian and Hesperian, the wet or dry crustal rheology
438 has a larger effect on the elastic thickness than the crustal temperature difference that results
439 from varying the mantle temperature by 200°C in the thermal evolution models and the choice of
440 the thermal evolution model itself. At the Hesperian/Amazonian boundary, constraints on crustal
441 rheology are weak due to large errors in the admittance elastic thickness. The effects of wet or
442 dry mantle rheology and the choice of the thermal evolution model itself are within the range of
443 observations. For the early plate tectonics and mantle overturn models, the effect of the crustal
444 thickness will be similar to the effect of crustal rheology, if the crustal thickness under southern
445 highlands is near or smaller than 60 km. Generally, the rheology of the crust is the crucial factor
446 influencing the elastic thickness.

447

448

449 **Relaxation of the dichotomy boundary**

450

451 For each thermal model, we predict the relaxation of the dichotomy boundary using
452 combinations of wet or dry mantle and crustal rheologies, and warm or cold mantle temperature
453 variations. Altogether, we calculated 24 models. Because of the uncertainty in the input
454 parameters, we distinguish only three stages of relaxation: relaxed, partially relaxed and not-
455 relaxed. This way the possible variation of the input parameters will not overly influence our
456 results.

457 All models using dry crustal rheology preserve the Martian dichotomy in its initial shape.
458 All models that use wet rheology in crust and mantle and warm temperature were not able to
459 preserve the Martian dichotomy. The models with both wet crust and mantle and cold
460 temperature show relaxation of a few km (see also Guest and Smrekar, 2005).

461 Figure 5 shows the final relaxation (at 3 Ga) of the models with wet crust and mantle and
462 cold temperature variation. The curves are compared to a MOLA topographic profile (Mission
463 Experiment Gridded Data Records, averaged from 4 pixels per degree to 1 pixel per degree)
464 perpendicular to the dichotomy boundary and centered at 60 E and 30 N. The relaxation for these
465 models is similar and fits well the topographic profile.

466 The models with wet crustal rheology and cold temperature variations fit best the
467 observed topography. However, because the initial shape of the dichotomy boundary is not
468 known, unrelaxed models could fit the topography of the boundary if we had chosen a different
469 initial shape. It was shown for some parts of the dichotomy boundary, e.g., the Ismenius Region
470 (Guest and Smrekar, 2005), that the boundary is partially relaxed and that a topographic slope
471 similar to 2° is needed to produce the observed faulting. In such a case only wet crustal rheology
472 allows for the partial relaxation of the boundary.

473

474

475 **Discussion**

476

477 The comparison between the modeled and admittance elastic thicknesses has major
478 implications for the rheology during the Noachian and the Hesperian in the southern hemisphere.

In the Noachian, the elastic thickness due to wet crustal rheology fits best the admittance elastic thickness of ~ 15 km in the Noachis, Cimmeria and Hellas regions, located in the central southern hemisphere. The elastic thickness is better fit with wet than dry crustal rheology for all three thermal models. The exception is the crust on the south rim of Hellas Basin that might have been wet or dry, which appears anomalous. The crust in Arabia Terra, apparently an eroded section of the highland crust located near the dichotomy boundary (Hynek and Phillips, 2001), was also wet in the Noachian. Since these regions cover most of the southern hemisphere, we conclude that the crust on the southern hemisphere was wet during the Noachian. The mantle rheology in the Noachian is unconstrained for the stagnant lid model because the elastic thickness is the same if wet or dry mantle rheology is used (see eq. 2). Wet mantle rheology gives a better fit for the other two models. Wet crust in the Noachian is also supported by results from relaxation modeling.

The only available admittance datum for the Hesperian is Solis Planum, located south of the Tharsis rise. The elastic thickness of 30-40 km is fit with wet crustal rheology for the stagnant lid model and slightly overestimated for other two models. Dry crustal rheology during the Hesperian does not fit admittance elastic thickness for any of the three thermal models. For the mantle, the wet rheology is preferred in the early Hesperian, in agreement with the thermal model of Hauck and Phillips (2002). Since Solis Planum is a single observation of this age, we cannot extend our conclusions globally.

The comparison of predicted and admittance elastic thickness at H/A boundary is not unique between the three thermal models. For the stagnant lid model at the H/A boundary (3 Ga), only models with dry crustal rheology fit the admittance elastic thickness while mantle rheology is unconstrained. For the early plate tectonics and mantle overturn models, both wet and dry

crustal and mantle rheologies fit the admittance elastic thickness due to the large uncertainties. Solis Planum, and Capri, Candor and Hebes Chasmata, are located in the vicinity of the Tharsis rise and therefore the same thermal evolution should apply for them. The admittance elastic thickness in Solis Planum in the Hesperian, 30-40 km, increases to 60-200 km in the Chasmata at the H/A boundary. For the stagnant lid model, crustal rheology would have to change from wet to dry in order to match the admittance thicknesses in Noachian and at H/A boundary. Thus we constructed a new model with a change of rheology from wet crust and mantle to dry crust and mantle at 3.5 Ga. The predicted elastic thickness is in agreement with admittance values (Figure 4a) and also the relaxation is very similar to the relaxation without rheology transition (Figure 5). Because these observations of the elastic thickness are restricted to the vicinity of the Tharsis, the change of rheology may be restricted to the vicinity of Tharsis as well. Globally dry crust and mantle at H/A boundary are contradictory to the presence of water in the crust and/or mantle implied from a 175 Ma old meteorite (McSween et al., 2001). Degassing of crust would probably require a change in global climate or remelting of the crust, which would lead to a different composition of the crust. There were some early suggestions from MGS that the northern plains contained andesite (Bandfield et al., 2000), but it is not consistent with more recent data from OMEGA, which shows that the north and south primarily differ in terms of the type of pyroxene present (Bibring et al., 2005). The early plate tectonics and mantle overturn models don't require but do allow for the change of rheology.

The crust below Alba Patera and the Elysium Rise, located in the northern hemisphere, was wet during the Hesperian/Amazonian based on the comparison between the model and admittance elastic thicknesses for early plate tectonics and mantle overturn models (Figure 4). For the stagnant lid model, the range of data fits both wet and dry crust. There seems to be a

contradiction of having relatively low elastic thickness in the northern and relatively high elastic thickness in the southern hemispheres during Hesperian-Amazonian. For the early plate tectonics and mantle overturn models it is possible to match both low and high data using wet crustal rheology and by constraining the crustal thickness on the southern hemisphere to ~ 60 km: then the high values on the southern hemisphere would reflect the rheology in the mantle whereas the low values on the northern hemisphere would reflect the rheology of the crust. Another possibility is that each hemisphere, or more precisely each studied region, differed in the amount of water in the crust. For the stagnant lid model, drying of the crust in the regions would allow to fit the data with higher elastic thickness.

The elastic thickness estimates helps us to constrain crustal thickness in these regions. The elastic thicknesses of the Elysium Rise and Alba Patera constrain the crustal thicknesses of the region to be >15 and >40 km, respectively, which is the minimum elastic thickness value. This is because the predicted elastic thickness with weakest rheology, the wet crust, is thicker than the admittance elastic thickness and thus no stronger rheology, e.g., mantle rheology, would fit the observations better.

We did not model the relaxation for the combination wet crust/dry mantle, however, we can roughly guess the elastic thickness evolution by combining the appropriate curves (wet crust up to 62 km, dry mantle over 62 km) on Figure 4. There is no better match of the values and the discussion for wet crust/wet mantle applies also for this case.

Our relaxation models that use wet crustal and mantle rheology and cold mantle temperatures show a good fit to the observed MOLA topography independently from the thermal model itself. This is because all these models have the same viscosity in the lower crust of 10^{20}-10^{21} Pas at 4-3.9 Ga (Figure 3) when most of the relaxation occurs. We tested the relaxation of

548 models where wet crustal and mantle rheologies change to dry at 3.5 Ga (Figure 5). As expected,
549 the relaxation is very similar to the relaxation without the rheology transition for both cold and
550 warm mantle temperatures. The models that use dry crustal rheology also preserve the Martian
551 dichotomy, however they overestimate the elastic thickness at 4 – 4.5 Ga more than the models
552 with wet crustal rheology. This is because the viscosity in the crust is higher then in the wet-crust
553 cases. If the temperature at the bottom of the lower crust is high enough, ~ 2000 K, to drop the
554 viscosity to the value of 10^{21} Pa s while using dry crustal rheology then the dichotomy will still
555 be preserved and the elastic thickness will decrease at least to the same value as it is for the wet
556 crust/cold temperature models in Noachian.

557 Our study attempts to distinguish between the three thermal evolution models. For each
558 thermal model, we discuss first the consequences of using a colder mantle temperature (~1550
559 K) than in the original models and then the possibility of a high temperature (~ 2000 K). For the
560 early plate tectonics model, the values as well as timing of the elastic-lithosphere thickening
561 predicted by our model fit well the admittance elastic thicknesses. The mantle and lower crustal
562 viscosity of 10^{20}-10^{21} Pa s at 4 Ga, which allows for the preservation of the Martian dichotomy,
563 is in good agreement with mantle viscosity used in the Breuer and Spohn (2003) thermal
564 evolution model. Breuer and Spohn (2003) used dry mantle rheology, whereas we use wet
565 mantle rheology and colder mantle temperature in order to achieve the same viscosity value. If
566 we accept an idea that entire crust was emplaced during an early plate tectonic epoch, than this
567 thermal evolution model is overall in good agreement with the relaxation and elastic thickness
568 modeling. If the plate tectonics ended earlier than 4 Ga, then temperature in the lithosphere
569 would be overall higher because the interior of the planet would have cooled less during the plate
570 tectonics regime. This is possible if plate tectonics acted very shortly, only 100-200 Myr.

571 For the stagnant lid model, the fit of the Noachian and Hesperian admittance values is the
572 best from all three models, but high H/A admittance values require a change of crustal rheology
573 from wet to dry, at least on the southern hemisphere. The mantle viscosity of 10^{19} Pa s was used
574 in order to produce the entire crust by ~ 4 Ga (Hauck and Phillips, 2002). Such a viscosity in the
575 lower crust however does not allow for preservation of the Martian dichotomy boundary. If
576 lower temperature is used in the thermal model, crustal production would slow down and would
577 not fit the observations. If a lower crustal viscosity of at least 10^{20} Pa s is used in our model
578 instead, along with a mantle viscosity of 10^{19} Pa s in concordance with the thermal model of
579 Hauck and Phillips (2002), the dichotomy boundary would be preserved. It is possible that the
580 creep parameters for wet crust are unrealistically weak due to the partial melting present in the
581 specimen (Mackwell et al., 1998). Varying creep parameters in the wet crustal creep law to
582 achieve a viscosity of 10^{20} Pa s causes the elastic thickness increases by ~ 5 km. The modeled
583 elastic thickness at 4 Ga would be around 25 km, which is 10 km more than admittance elastic
584 thickness, which is probably still within the error of the admittance elastic thickness. If we accept
585 the change of crustal rheology, then this model would be in a good agreement with the
586 observations. The temperature of ~2000 K implies at least 200 km thick crust formed by 4.4 Ga
587 which is too thick in order to preserve the dichotomy. Also, the predicted elastic thickness would
588 not fit the values at the H/A boundary even for the dry rheology (shift the curve for dry rheology
589 to start at 4.4 Ga on Figure 4). The dry rheology could be ruled out for this model.

590 For the mantle overturn model, the amount of the elastic-lithosphere thickening predicted
591 by our model is in good agreement with the estimates from gravity and topography if we use the
592 initial condition as shown on Figure 1 and place the beginning to 4 Ga. Then the curves of elastic
593 thickness can be simply shifted along the time axes and the same results would imply. However,

lower mantle temperature is in disagreement with the thermal profile after overturn and therefore we explore the possibility of a high initial temperature for mantle overturn model. We use an earlier mantle overturn model (Elkins-Tanton et al., 2003) where initial thermal profile was not corrected for partial melting and we assume that the crust was emplaced at once near the surface and no cooling has occurred during the emplacement. Such a thermal profile represents the hottest variant of the mantle overturn model and ensures temperature high enough to achieve the vicsosity of 10^{21} Pas in the lower crust (Figure 6) when using dry crustal rheology. Such a case allows for the preservation of the dichotomy as well as it fits the best the admittance elastic thickness in Noachian: the elastic thickness is 2 km at 4.4 Ga (Figure 6). This case also fits well the highest values at H/A boundary, as well as the anomalous S. Hellas Rim with intrusions, however it does not fit the value for Solis Planum in Hesperian and the Alba Patera and Elysium Rise values. In order to fit the elastic thickness in Solis Planum, an event that would increase temperature and significantly weakened the rheology of the crust by water or maybe melting would be necessary in the close proximity of Solis Planum so that it does not influence the elastic thickness of other Noachian terrains. This may also apply to Alba Patera and Elysium Rise. This implies that the crust in the southern hemisphere was and remains dry, and was significantly perturbed with local upwelling of hot and wet material from the mantle during Hesperian. The northern hemisphere was locally perturbed or globally wet at least at H/A boundary. This, in fact, is a scenario suggested for Amazonian volcanoes (Solomon and Head, 1990; McGovern et al., 2004) and therefore should not be ruled out. The same scenario may apply to stagnant lid and plate tectonics model.

As mentioned before, the hot temperature, as used in Figure 6 is in good agreement with the original model. Because this model is based on the conductive cooling of the inverse thermal

profile, it is possible that mantle convection would significantly warm up the lithosphere. Based on the contemporary numerical models, mantle convection would not start till 100-300 Myr after the overturn (Zaranek and Parmentier, 2004) if the mantle viscosity is around ~10^{18} Pa s. Most of the relaxation would have occurred by then and therefore possible mantle convection should not influence the relaxation. However, the convection might initially warm up the lithosphere and the crust for a short period of time (Zaranek and Parmentier, 2004) and thus, if long enough, alter the relaxation and the elastic thickness results. More numerical modeling is necessary to resolve this issue.

In order to distinguish between the models, additional constraints are necessary. These constraints would be more precise values of the admittance elastic thickness with tighter timing constraints and geochemical constraints on water content of the crust. The most problematic admittance values are for Solis Planum and the S. Hellas rim. None of the models can fit both of these values – dry crustal rheology fits S. Hellas rim whereas wet crustal rheology fits Solis Planum - and therefore one or both must have experienced a unique geologic history.

Hydrothermal cooling (Solomon et al., 2005, Parmentier and Zuber, 2006), which is not considered in our calculations, will have some effect on preservation of the dichotomy boundary and evolution of the elastic thickness. The presence of a brecciated and thus lower thermal conductivity layer in the upper crustal layer would increase the temperature in and thus relaxation of the lower crust. Alternatively, if groundwater convection occurs in the brecciated upper crustal layer, it would cool both the upper and lower crusts and slow down the relaxation (Parmentier and Zuber, 2006). Although the presence of hydrothermal cooling in our model would slow down the relaxation and preserve the Martian dichotomy, it would also cause too

large an increase in the elastic thickness in the Noachian and Hesperian to be in agreement with admittance values.

The crustal thickness has a strong influence on the elastic-thickness evolution because of the change of the rheology between the crust and mantle. If the crustal thickness is thinner than 62 km in our model, the wet crustal rheology would change to stronger mantle rheology at shallower depth and would increase the elastic thickness earlier than in the present models. This could provide a better fit to the admittance elastic thickness for the stagnant lid model. However, the crustal thickness under the highlands would have to be around 40 km, which is probably unrealistic. A thicker crust would influence results in the early plate tectonics and mantle overturn models. A thicker crust would result in a smaller elastic thickness of approximately 60-70 km at H/A boundary for both models. Given the large errors on admittance elastic thickness estimates at the H/A boundary, results for both a nominal and a thick crust fit the observations.

Generally, the strong increase in the admittance elastic thickness of at least 100 km between 4 and 3 Ga can be explained by an increase in lithospheric strength due to either cooling or a loss of water from the crust. Because the admittance elastic thicknesses are located on the volcanic province of Tharsis, the water loss from the crust due to volcanic activity is a possible scenario, supported by the amount of volcanic activity (Greeley, 1987), by dating of eroded channels (Phillips et al., 2001), and by the sedimentary record (Poulet et al., 2005). However, degassing likely requires remelting of the crust and an evolved crustal composition, which is not observed. There is a difference in the admittance elastic thickness between major volcanic provinces, the Tharsis rise region (~ 100 km, Amazonian surface age), and Alba Patera and Elysium rise regions (20-60 km, Hesperian to Amazonian surface age). The difference can be attributed to the different ages (age is not well constrained) of the regions, local variations in

662 temperature (McGovern et al., 2004), or local variations in the crustal water content. We note
663 that while there is no evidence of evolved and thus potentially dry crust, the large elastic
664 thicknesses for volcanic provinces may actually reflect mantle elastic support. The huge amount
665 of volcanism in these regions, and in Tharsis in particular, may have created a dry mantle.
666
667 **Conclusions**
668
669 We have used three thermal evolution models for Mars, stagnant lid, early plate tectonics
670 followed by stagnant lid, and mantle overturn, calculated with two different mantle temperatures
671 along with wet and dry rheologies, to predict the temperature and viscosity evolution of the
672 lithosphere. These viscosities are then used to predict the relative amount of relaxation of the
673 global dichotomy and elastic thickness values from the Noachian to the Hesperian/Amazonian.
674 The thermal models predict three distinct lithospheric cooling scenarios. The stagnant lid
675 model starts with the coolest lithosphere, but does not cool as efficiently as the other two models.
676 This causes the relaxation of the Martian dichotomy to be the slowest of the three models and the
677 elastic thickness to increase the least over time. Both the early plate tectonics and mantle
678 overturn models cool very efficiently, even though the mantle temperature evolutions differ
679 significantly. This causes a strong increase in the elastic thickness in these models but occurs too
680 late to significantly change the amount of relaxation of the Martian dichotomy. All three thermal
681 models can preserve the long-wavelength topography of Mars while relaxing the short
682 wavelengths if the viscosity in the lower crust is 10^{20}-10^{21} Pas during the first 0.1 Ga after
683 formation of dichotomy.

Our modeling shows that in Noachian and Hesperian, wet or dry crustal rheology has a larger effect on the elastic thickness than the crustal temperature difference that results from varying the mantle temperature by 200°C and the choice of the thermal evolution model itself. Similarly, wet/dry crustal rheology also has a major effect on the relaxation of the Martian dichotomy.

The elastic thickness modeling and additional constraints can be used in order to distinguish between the thermal models. For the stagnant lid model, wet crust at 4 Ga that changes to dry crust by the H/A boundary with cold temperatures are the best match.. A loss of water from the crust implies remelting and evolved crustal composition, which is not confirmed by observations. A transition to a drier atmosphere could also enhance outgassing. In this scenario, the S. Hellas Rim with intrusion would be anomalous unless explained by a local event. Interestingly, this region and the chasmata are the only regions that use bottom loading in the admittance modeling, which might be connected with melting and thus a drying mechanism. However, the colder mantle temperature, necessary for this model, is probably not realistic and would not produce the desired volume of crust based on Hauck and Phillips (2002) results.

The early plate tectonics model works the best with the change to stagnant lid regime at 4 Ga. For this case, the wet crust and colder temperature profile together with a crustal thickness of ~ 50-60 km under highlands can explain all admittance elastic thicknesses except the S. Hellas Rim with intrusion. If the crustal thickness is higher, then a change of crustal rheology from wet to dry would be required. If plate tectonics ended by ~4.4 Ga, then dry crustal rheology through out would be possible in order to preserve the dichotomy. Then Solis Planum, Alba Patera and Elysium Rise would be anomalously wet crust. Alba Patera and Elysium Rise are located on the

706 northern hemisphere suggesting a possibility of a different crustal water content on the northern
707 hemisphere.

708 Mantle overturn probably occurred in the early history of Mars, i.e. by 50 Myr. This
709 model is sensitive to the initial thermal conditions. If we assume fast emplacement of the crust
710 then dry crustal rheology provides the best match. Similarly to the early plate tectonics model,
711 Solis Planum, Alba Patera and Elysium rise would be anomalously wet. The same consequences
712 as for the early plate tectonics apply. If however an initial thermal condition includes some
713 initial cooling then wet crustal rheology will provide the best match. In this case, all data are
714 matched except the S. Hellas Rim with intrusion. The only problem is that the colder temperature
715 might disagree with the idea of the mantle overturn.

716 For all thermal models, the mantle rheology will be constrained to be wet if elastic
717 thickness in the Hesperian is in range 30-40 km, as determined so far for Solis Planum.

718

719

720

721 Acknowledgements. This work was supported by a grant from the Mars Data Analysis
722 Program. We thank Sean Solomon for his comments on Martian rheology. We thank Linda
723 Elkins-Tanton and Patric J. McGovern for constructive comments that helped to improve the
724 manuscript.

725

726

727 **References**

728

729 Bandfield, J. L., Hamilton, V. E., and Christensen, P. R., 2000. A global view of Martian Surface
730 compositions from MGS-TES, Science, 287, 1626 – 1630.
731
732 Belleguic, V., Lognonne, P., and Wieczorek, M., 2005. Constraints on the Martian lithosphere
733 from gravity and topography data, J. Geophys., Res., 110, doi:10.1029/2005JE002437.
734
735 Bibring, J.P., Langevin,Y., Gendrin, A., Gondet, B., Poulet, F., Berthé, M., Soufflot, A.,
736 Arvidson, R., Mangold, N., Mustard, J., Drossart, P., and the OMEGA team, 2005. Mars Surface
737 Diversity as Revealed by the OMEGA/Mars Express Observations, Science, 10.1126/ 1108806
738
739 Breuer, D., and Spohn, T., 2003. Early plate tectonics versus single-plate tectonics on Mars:
740 Evidence from magnetic field history and crust evolution, J. Geophys. Res., 108, doi:
741 10.1029/2002JE001999.
742
743 Burov, E. B., and Diament, M., 1995. The effective elastic thickness (Te) of continental
744 lithosphere: What does it really mean?, J. Geophys. Res., 100: 3905-3927.
745
746 Caristan, Y. , 1982. The transition from high temperature creep to fracture in Maryland diabase,
747 J. Geophys. Res., 87: 781-6790.
748
749 Cathles, L. M., 1975. Viscosity of the Earth's mantle, Princeton University Press, Princeton, N.
750 J., 386 pp.
751

752 Connerney, J.E., Connerney, E. P., Acuña, M. H., Wasilewski, P. J., Ness, N. F., Rème, H.,
753 Mazelle, C., Vignes, D., Lin, R. P., Mitchell, D. L., Cloutier, P. A. et al., 1999. Magnetic
754 Lineations in the Ancient Crust of Mars. Science, 284: 794-798.
755
756 Dombard, A. J., Phillips, R. J., 2005. Tectonic Evidence for Crustal Underplating of the Tharsis
757 Montes, Mars, LPSC Abstract, no.1878, 2005LPI, 36.1878D.
758
759 Elkins-Tanton L.T.; Parmentier E.M.; Hess P.C., 2003. Magma ocean fractional crystallization
760 and cumulate overturn in terrestrial planets: Implications for Mars. Meteoritics and Planetary
761 Science, 38, 1753-1771.
762
763 Elkins-Tanton, L. T., Hess, P. C. and Parmentier, E. M., 2005. Possible formation of ancient
764 crust on Mars through magma ocean processes. J. Geophys. Res., 110: E12S01,
765 doi:10.1029/2005JE002480.
766
767 Frey, H. V., Sakimoto, S. E., and Roark, J., 1998. The MOLA topographic signature at the
768 crustal dichotomy boundary zone on Mars, Geophys. Res. Let., 25: 4409-4412.
769
770 Frey, H. V., 2006. Impact constraints on the age and origin of the lowlands of Mars, Geophys.
771 Res. Letters, 33, doi:10.1029/2005GLo24484.
772
773 Greeley, R., 1987. Release of Juvenile Water on Mars: Estimated Amounts and Timing
774 Associated with Volcanism, Science, 236: 1653-1654.

775

776 Grimm, R. E., and Solomon, S. C., 1988. Viscous relaxation of impact crater relief on Venus:
777 Constraints on crustal thickness and thermal gradient, J. Geophys. Res., 93: 1911-1929.

778

779 Guest, A., and Smrekar, S. E., 2005. Relaxation of Martian Dichotomy Boundary:
780 Faulting in the Ismenius Region and Constraints on the Early Evolution of Mars. J.
781 Geophys. Res., 110: E12S25, doi: 10.1029/2005JE002504.

782

783 Hartmann W. K., and Neukum, G., 2001. Cratering Chronology and the Evolution of Mars, Space
784 Science Reviews, 96, 165-194.

785

786 Hauck II, S. A., and Phillips, R. J., 2002. Thermal and crustal evolution of Mars, J. Geophys.
787 Res. 107: 10.1029/2001JE001801.

788

789 Hoogenboom, T., and Smrekar, S. E., 2006. Elastic thickness estimates for the northern lowlands
790 of Mars, Earth and Planet. Sci. Lett., 248, 830-839.

791

792 Hynek B. M., and Phillips R. J., 2001. Evidence for extensive denudation of the Martian
793 highlands. Geology, 26: 407-410.

794

795 Jakosky, B. M., and Phillips, R. J., 2001. Mars' volatile and climate history. Nature 412: 237-
796 244.

797

798 Karato, S-I., and Wu, P., 2001. Rheology of the Upper Mantle: A Synthesis, Science, 260: 771-
799 778.
800
801 Lenardic, A., Nimmo, F., and Moresi, L., 2004. Growth of the hemispheric dichotomy and the
802 cessation of plate tectonics on Mars, J. Geophys. Res., 109: doi: 10.1029/2003JE002172.
803
804 Mackwell, S. J., Zimmerman, M. E., and Kohlstedt, D. L., 1998. High-temperature deformation
805 of dry diabase with application to tectonics on Venus, J. Geophys. Res., 103: 975-984.
806
807 McGill, G. E., and Dimitriou, A. M., 1990. Origin of the Martian global dichotomy by crustal
808 thinning in the late Noachian or early Hesperian, J. Geophys. Res., 95: 12,595-12,605.
809
810 McGovern P. J., Solomon, S. C., Smith, D. E., Zuber, M. T., Simons, M., Wieczorek, M. A.,
811 Phillips, R. J., Neumann, G. A., Aharonson, O., and Head, J. W., 2002. Localized
812 gravity/topography admittance and correlation spectra on Mars: Implications for regional and
813 global evolution, J. Geophys. Res., 107, 5136: doi: 10.1029/2002JE001854.
814
815 McGovern P. J., Solomon, S. C., Smith, D. E., Zuber, M. T., Simons, M., Wieczorek, M. A.,
816 Phillips, R. J., Neumann, G. A., Aharonson, O., and Head, J. W., 2004. Correction to "Localized
817 gravity/topography admittance and correlation spectra on Mars: Implications for regional and
818 global evolution", J. Geophys. Res., 109: 5136, doi: 10.1029/2004JE002286
819

McSween, H.Y. Jr, Grove, T.L., Lentz, R.C., Dann, J.C., Holzheid, A.H., Riciputi, L.R., Ryan, J.G., 2001. Geochemical evidence for magmatic water within Mars pyroxenes in the Shergotty meteorite. Nature, 409: 487-490.

Neumann, G. A., Zuber, M. T., Wieczorek, M. A., McGovern, P. J., Lemoine, F. G., Smith, D. E., 2004. The crustal structure of Mars from gravity and topography, J. Geophys. Res., 109: doi:10.1029/2004JE002262.

Nimmo, F., 2005. Tectonic consequences of Martian dichotomy modification by lower-crustal flow and erosion. Geology, 33(7): 533-536.

Nimmo, F., and Stevenson, D. J., 2000. Influence of early plate tectonics on the thermal evolution and magnetic field of Mars. J. Geophys. Res., 105: 11969.

Nimmo, F., and Stevenson, D. J., 2001. Estimates of Martian crustal thickness from viscous relaxation of topography, J. Geophys. Res., 106: 5085-5098.

Parmentier, E. M., and Zuber, M. T.2006. Early evolution of Mars: Mantle compositional stratification or hydrothermal crustal cooling? Submitted to J. Geophys. Res.

Petit, C., and Ebinger, C.,2000. Flexure and mechanical behavior of cratonic lithosphere: gravity models of the East African and Baikal Rifts, J. Geophys. Res., 15: 19151-19162.

Phillips, P.M.A., 2001. Ancient geodynamics and global-scale hydrology on Mars. Science, 291: 2587-2591.

Poulet, F., Bibring, J.-P., Mustard, J. F., Gendrin, A., Mangold, N., Langevin, Y., Arvidson, R. E., Gondet, B., Gomez, C., and the Omega Team, 2005. Phyllosilicates on Mars an dimplications for early martian climate. Nature, 438: 623-627.

Solomon, S. C. and Head, J. W., 1990. Heterogeneities in the thickness of the elastic lithosphere of Mars – Constraints on heat flow and internal dynamics, J. Geophys. Res., 95: 11073-11083.

Solomon, S.C., 2005. New perspectives on ancient Mars. Science, 307(5713): 1214-1220.

Spohn, T., Acuña, M. H., Breue, D., Golombek, M., Greeley, R., Halliday, A., Hauber, E., Jaumann, R., and Sohl, F., 2001. Geophysical Constraints on the Evolution of Mars. Space Science Reviews, 96: 231-262.

Tanaka, K.L., Scott, D.H., and Greeley, R., 1992. Global stratigraphy, in Mars, edited by H. H. Kieffer et al. (Ed.), pp. 1455, Univ. Ariz. Press, Tucson.

Turcotte, D. L., and Schubert, G., 2002. Geodynamics, 2nd edition, p. 456, Cambridge University Press, New York.

865 Zaranek, S. E., and Parmentier, E. M., 2004. Convective cooling of an initially stably stratified
866 fluid with temperature-dependent viscosity. J. Geophys. Res., 109: B03409.
867
868 Zhong, S., 1997. Dynamics of crustal compensation and its influences on crustal isostasy, J.
869 Geophys. Res., 102: 15,287-15,299.
870
871 Zhong, S., and M. T. Zuber, 2000. Long-wavelength topographic relaxation for self-gravitating
872 planets and its implications for the time-dependent compensation of surface topography, J.
873 Geophys. Res. 105: 4153-4164.
874
875 Zuber, M.T., 2000. Internal structure and early thermal evolution of Mars from Mars Global
876 Surveyor topography and gravity. Science, 287(5459): 1788-1793.Global Surveyor topography
877 and gravity, Science, 287: 1788-1793.
878

879 **Figure Captions**

880

881

882 Figure 1: Three thermal evolution models of the lithosphere: a) stagnant lid, b) early plate
883 tectonics, and c) mantle overturn, shown by a solid line (termed "warm" in the text). The coldest
884 profile corresponds to 4 Ga, the warmest profile corresponds to 3 Ga. The dashed lines show a
885 cooler variant of each model (termed "cold" in the text) in which the mantle temperature is 200
886 K cooler than that in the warm model.

887

888 Figure 2: Sketch of the semi-analytical model to the depth of 80 km. Horizontal size of the model
889 is 4500 km, but only the central third is shown. The initial topography is slightly higher and
890 steeper than present-day dichotomy topography. The topography is isostatically compensated
891 (Airy model) by a crustal root (density is 2900 kg/m^3) at the crust/mantle boundary (the density
892 difference is 600 kg/m^3).

893

894 Figure 3: Time evolution of viscosity used in the relaxation models: a) stagnant lid, b) early plate
895 tectonics, and c) mantle overturn thermal models. Solid lines – warm thermal model; dashed
896 lines – cold thermal model; green lines – wet mantle rheology; blue lines – dry mantle rheology;
897 blue line with red dots – dry lower crustal rheology. Note that for stagnant lid and early plate
898 tectonics, the green dashed line is overlapped by the solid blue line, meaning that the mantle
899 viscosity for dry warm mantle and wet cold mantle are essentially the same. When wet rheology
900 is used, the same viscosity is used in the lower crust and mantle.

901

Figure 4: Comparison between modeled and admittance elastic thicknesses for a) stagnant lid, b) early plate tectonics, and c) mantle overturn thermal models. The left vertical axis corresponds to the age of the modeled elastic thickness whereas the right vertical axis shows the surface age of the admittance elastic thickness. N- Noachian, H – Hesperian, N-H – overlapping Noachian and Hesperian, H-A – overlapping Hesperian and Amazonian epochs. The modeled elastic thickness is shown by solid (warm thermal model) and dashed (cold thermal model) lines of green (wet crustal and mantle rheology), blue (dry crustal and mantle rheology), magenta (dry crust and wet mantle), and red (wet crustal and mantle rheology changes to dry rheologies at 3.5 Ga) colors. When wet crustal rheology is used, two elastic layers develop; then green lines show the elastic thickness in the crust (h1), while magenta lines deeper than base of the crust (62 km) show the elastic thickness in the wet mantle (h2). The effective thickness, shown by empty (cold thermal model) and full (warm thermal model) triangles, is determined using equation 2. The admittance elastic thickness, taken from McGovern et al. (2004), is shown by black bars. Within a given age subdivision, vertical positions give an approximate indication of the relative surface ages of features (McGovern et al., 2004) and has no relation to the age shown on the left axis. The elastic thickness for Noachian northern plains (Hoogenboom and Smrekar, 2006) is shown by blue bars and for Alba Patera and Elysium rise (Belleguic et al., 2005) by purple bars.. The age of the epoch's boundaries is based on Hartman and Neukum (2001). The black double headed arrow on top of the figures show the crustal thickness of the northern plains ("NP") and southern highlands ("SH"). The triangle shows the average crustal thickness of 62 km. The elastic thickness smaller than 62 km is based on the crustal rheology whereas the one larger than 62 km is based on mantle rheology.

925 Figure 5: Results from semi-analytical relaxation modeling. The initial shape at 4 Ga, the relaxed
926 shape at 3 Ga (thin lines), and present MOLA topography profile through the dichotomy
927 boundary (thick line) are compared. The models with 62 km thick crust, cold mantle and initial
928 wet crustal and mantle rheology are shown: solid line – stagnant lid model; long dashes – the
929 same, but rheology changes to dry at 3.5 Ga; dots – early plate tectonics model; short dashes –
930 mantle overturn model. MOLA topographic profile is averaged over 10 degree wide swath
931 centered at 30 N and 60 E and perpendicular to the dichotomy boundary.
932
933
934 Figure 6: a) Thermal evolution, b) viscosity, c) elastic thickness evolution and d) topographic
935 relaxation for mantle overturn model assuming fast emplacement of the crust. The legend is the
936 same as on a) Figure 1, b) Figure 3, c) Figure 4, d) Figure 5.
937

Table 1: Creep laws

Strain rate for wet diabase[a]	$=0.0612\sigma^{3}\exp(-276000/R/T)$
Strain rate for dry diabase[b]	$=8.0\sigma^{4.7}\exp(-485000/R/T)$
Strain rate for wet olivine[c]	$=2.0*10^{18}(\sigma/G)^{3}\exp(-(430000+15*3100)/R/T)$
Strain rate for dry olivine[c]	$=3.5*10^{22}(\sigma/G)^{3.5}\exp(-(540000+20*3100)/R/T)$

[a][Caristan, 1982]

[b] [Mackwell et al., 1998]

[c] [Karato and Wu, 1993]

σ is the deviatoric stress, in MPa

T is temperature, in K

G is rigidity, in MPa

R is gas constant, equals 8.314 J $mole^{-1}$ K^{-1}

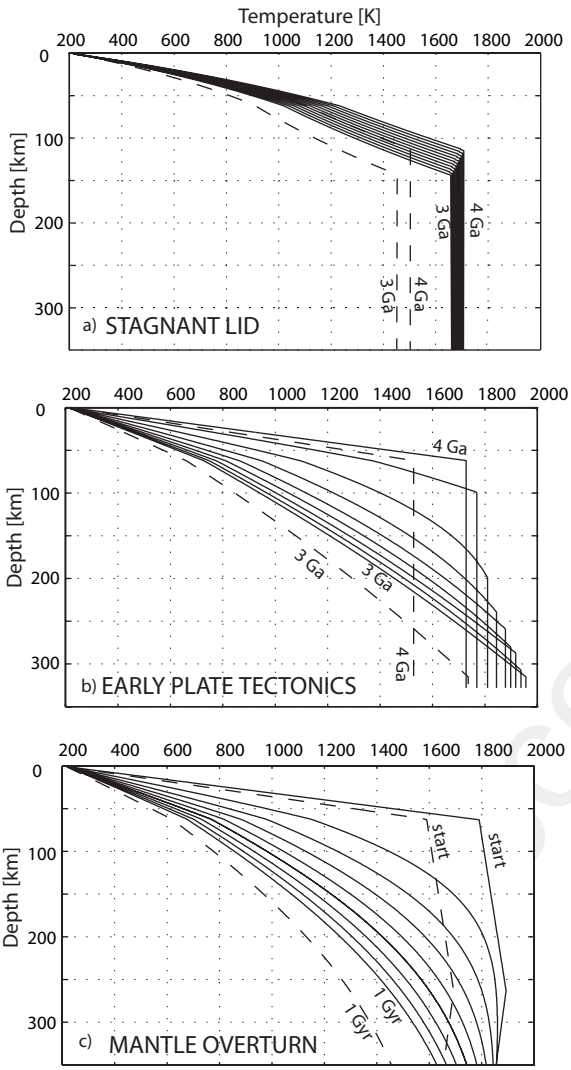

Fig1.ai

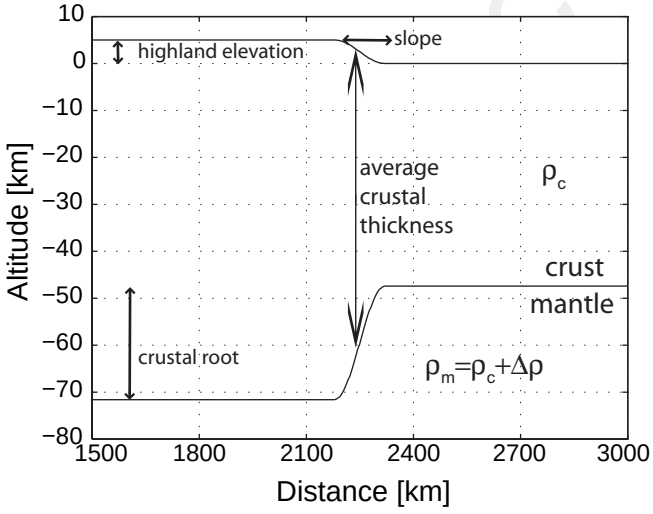

fig2.ai

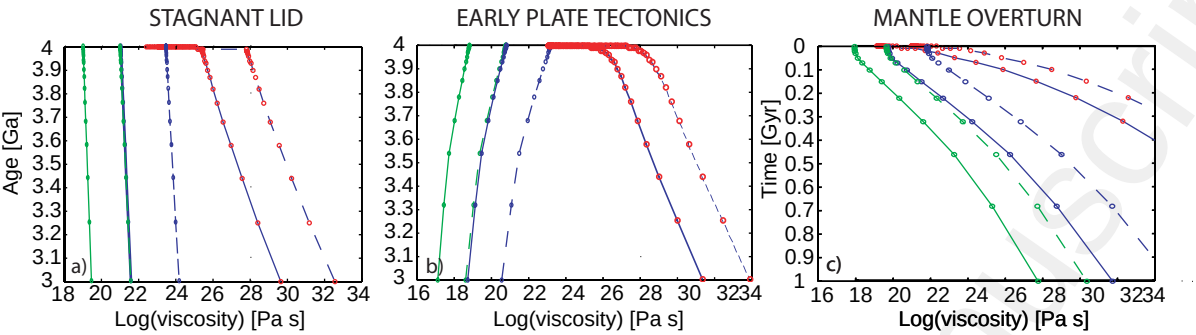

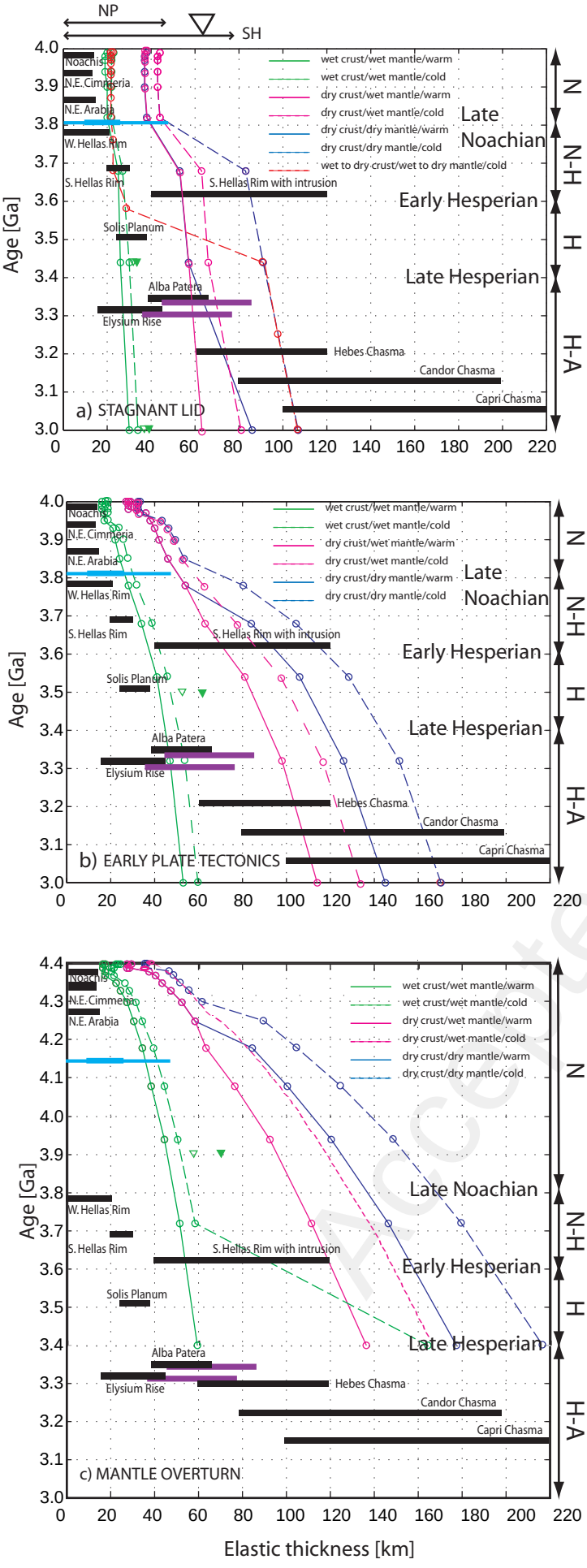

fig4.ai

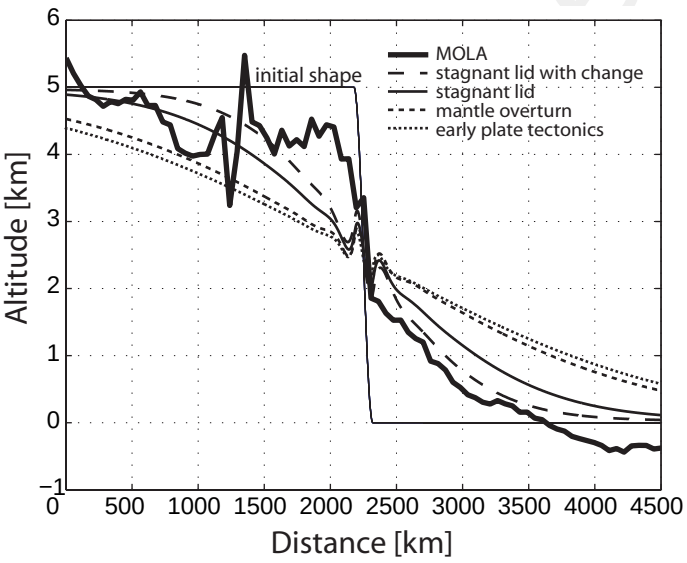

fig5.ai

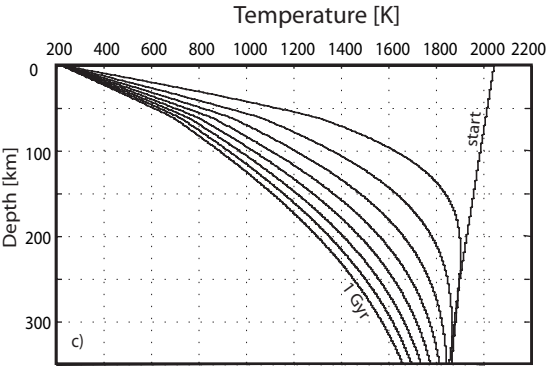

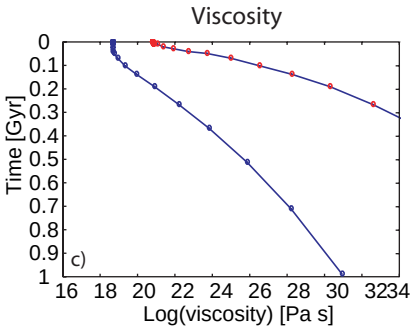

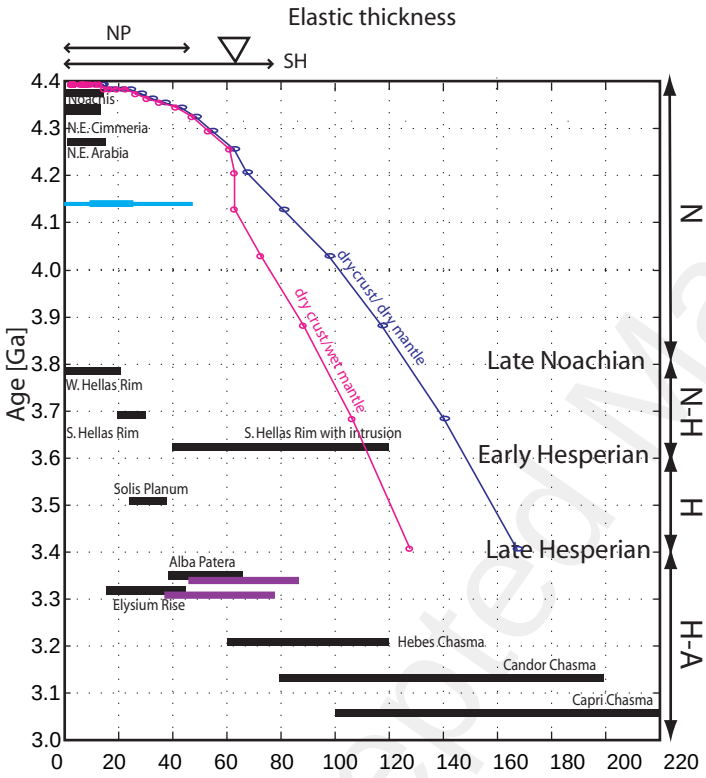

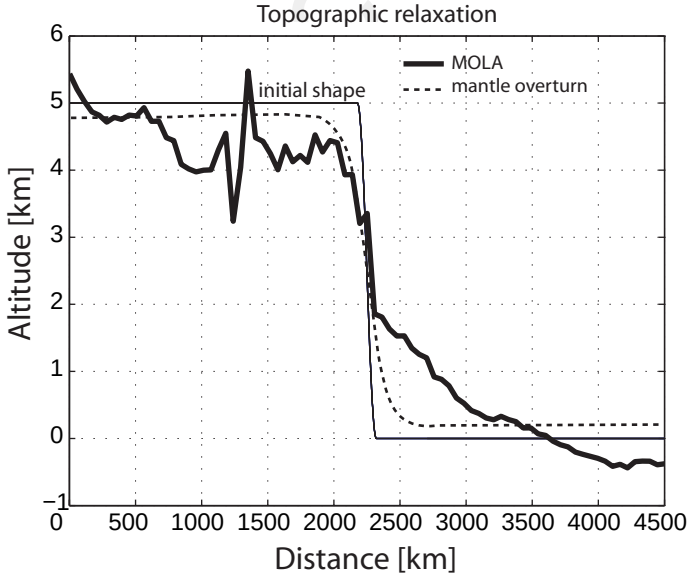

fig6.ai